JOURNAL OF VIROLOGY, Dec. 1996, p. 8675–8683 Vol. 70, No. 12
0022-538X/96/$04.00+0


# Reversible Dissociation of the Poliovirus Replication Complex: Functions and Interactions of Its Components in Viral RNA Synthesis

DENISE EGGER, LUIS PASAMONTES,† ROGER BOLTEN, VITALY BOYKO, AND KURT BIENZ*

*Institute for Medical Microbiology, University of Basel, Basel, Switzerland*

Received 8 July 1996/Accepted 5 September 1996

**Membrane-bound replication complexes containing transcriptionally active replicative intermediates (RI) can be isolated from poliovirus-infected HEp-2 cells and consist of rosette-like structures of virus-induced vesicles surrounding the replicating viral RNA. At low ionic strength and low temperature, the rosettes reversibly dissociate into individual tubulated vesicles. As determined by immunoelectron microscopy and immunoprecipitation, the vesicles carry a set of viral structural and nonstructural proteins as well as RI RNA. At 30°C, the vesicles reassociate into rosettes synthesizing plus-strand RNA in the RI. The in vitro transcriptional activities of rosettes and vesicles kept separated by high dilution were assessed by an RNase protection assay. The synthesis of the first 178 nucleotides at the 5′ end of the plus strand was considered to reflect initiation, and the detection of a 530-nucleotide fragment in the P2 genomic region was considered to reflect elongation. It could be shown that the initiation and elongation of plus strands on individual vesicles are comparable to those in rosettes, with initiation proceeding in de novo-assembled initiation complexes. By use of detergent treatment it was found that initiation, but not elongation, is dependent on vesicular membranes.**

During replication of poliovirus RNA, plus-strand genomic RNA is copied by the viral polymerase $3D^{pol}$ (4, 19, 55) into minus-strand RNA, which acts as a template for the synthesis of progeny plus strands in the replicative intermediate (RI) (21). Plus-strand synthesis depends on specialized cellular membraneous structures (12, 16, 18, 39), whereas the intracellular structural prerequisites for minus-strand RNA synthesis are not known. Virtually all noncapsid proteins, i.e., the P2 (7, 14, 26, 30, 36, 52, 56) as well as the P3 proteins (2, 3, 20, 23, 27, 35, 41, 55), in addition to cellular factors (2, 33, 47), seem to be involved in plus-strand synthesis.

The RI-dependent plus-strand RNA synthesis proceeds in a viral replication complex (reviewed in reference 10) which was identified by electron microscopy (9, 13) and found to be located on the surfaces of virus-induced cytoplasmic vesicles. The intracellular formation of these vesicles has been attributed to the viral protein 2BC (13). These vesicle-inducing and membrane-altering properties of 2BC have been recently confirmed by expressing recombinant P2 proteins 2BC and 2C in cultured cells (1, 17). The altered membranes of poliovirus-infected cells have been found to be of multiorganelle origin, including the rough endoplasmic reticulum as well as the Golgi complex (49).

Upon isolation from infected cells, the virus-induced vesicles were found to form rosettes which surround the replication complex (12). The vesicular rosettes can be isolated in a functional state, and the rosettes continue to initiate (51) and elongate and release (11, 14, 51) progeny plus-strand RNA in an in vitro transcription system. Such systems rely on the preformed structures isolated from infected cells and thus are different from the recently described cell-free translation-transcription systems, which are reconstituted from uninfected cells and programmed with virion RNA (5, 6, 37, 38).

In investigating the structure of the rosette and the nature of the association of the viral RNA with components of the rosette, it was found that only mature progeny plus-strand RNA is present on the surface of the rosette (11), whereas the actual RNA-synthesizing machinery is tightly enclosed and protected in the interior of the rosette (11). This arrangement impedes to a large extent the in situ investigation of the architecture of the rosettes. In the present study, in trying to characterize the individual components of the functional replication complex, we found that rosettes can reversibly be dissociated into their components, i.e., the virus-induced vesicles, and reassociated into rosettes. This proved to be helpful in elucidating some of the structural and functional features of the viral replication complex. It was found that the vesicles undergo extensive tubulation on their side facing the center of the rosette. They carry sets of nonstructural and capsid proteins as well as an RI which was found to be attached to the surface of individual vesicles. Vesicles reassociate into rosettes which synthesize viral RNA in the RI. By using an RNA protection assay, it was possible to demonstrate that initiation of plus-strand RNA synthesis as well as elongation of viral RNA can take place not only in rosettes but also on single vesicles. Individual vesicles, therefore, are equipped for initiation and elongation and can sustain the transcriptional activity of the viral RI.

## MATERIALS AND METHODS

**Cells, virus, and isolation of the replication complex containing rosettes.** HEp-2 cells and poliovirus type 1 (Mahoney) were grown in suspension cultures. The multiplicity of infection for the experiments was 30 PFU per cell. The preparation of cytoplasmic extracts and the isolation of the vesicle-attached replication complexes (rosettes) was as published previously (14). In short, cytoplasmic extracts were centrifuged onto a double sucrose cushion (30 and 45% sucrose), and the band on the 30% sucrose was harvested (30% sucrose fraction).

**In vitro RNA synthesis and dissociation and reassociation of rosettes.** The 30% sucrose fractions were stored at −70°C. For the experiments, suitable aliquots were thawed, and 7 to 10 μl was added directly to 40 μl of an in vitro RNA-synthesizing system as described previously (14, 51). To dissociate rosettes into single vesicles, rosettes were diluted 1:3 with water before or 1:10 with 10

* Corresponding author. Mailing address: Institute for Medical Microbiology, University of Basel, Petersplatz 10, CH-4003 Basel, Switzerland. Phone: 41-61 267 3290. Fax: 41-61-267 3298. Electronic mail address: BIENZ@ubaclu.unibas.ch.

† Present address: F. Hoffmann-La Roche AG, Vitamin Research Biotechnology 64/7, CH-4070 Basel, Switzerland.

mM Tris (pH 7.4) after in vitro transcription and kept at 0°C for 15 min. Reassociation to functional rosettes occurred spontaneously at 30°C. Association or dissociation of rosettes was tested by electron microscopy (EM).

**Analysis of in vitro-synthesized viral RNA.** For analysis of the in vitro-synthesized RNA, 35 μCi of [5,6-$^3$H]UTP (Amersham International, Little Chalfont, United Kingdom) was added to 40 μl of the transcription system. After phenol-chloroform-isoamyl alcohol (25:24:1) extraction and ethanol precipitation, RNA was analyzed in a 1% agarose gel (Bethesda Research Laboratories, Gaithersburg, Md.) under nondenaturing conditions at 40 V on ice. For fluorography, the gels were impregnated with En$^3$Hance (E.I. Dupont de Nemours, Boston, Mass.), dried, and exposed on Kodak X-Omat film at −70°C for 1 to 2 days.

Alternatively, RNA was denatured in formamide and formaldehyde by heating for 10 min at 68°C and then run at 50 V on a formaldehyde-containing 0.8 or 1% agarose gel. For hybridization, the gel was blotted onto a Biodyne A nylon membrane (Pall, Portsmouth, United Kingdom) in 20× SSC (1× SSC is 0.15 M NaCl plus 0.015 M sodium citrate). After prehybridization for 1 h at 55°C, hybridization was performed overnight at 55°C in a buffer containing 50% formamide, 5× SSC, 5% blocking reagent (Boehringer, Mannheim, Germany), 0.01% Na *N*-lauroyl sarcosinate, and 0.02% sodium dodecyl sulfate (SDS). RNA probes were labeled with digoxigenin-11-UTP (DIG) (Boehringer) by in vitro transcription with SP6 or T7 polymerase (Boehringer) from the corresponding DNA template which had the SP6 or T7 promoter added by PCR (50, 58). The probe was detected with anti-DIG antibody coupled to alkaline phosphatase (Boehringer) with nitroblue tetrazolium–5-bromo-4-chloro-indolylphosphate toluidinium as a color reagent.

**RNase protection assay to demonstrate initiation and elongation.** To test for synthesis of newly initiated viral plus-strand RNA and for elongation of plus strands in rosettes or vesicles, viral RNA was pulsed with 0.5 to 1.75 μCi of [$^{35}$S]UTP (Amersham) per μl, phenol-chloroform-isoamyl alcohol extracted, and subjected to an RNase protection assay. For this assay, unlabeled riboprobes of minus polarity, spanning nucleotides (nt) 1 to 178 and 4124 to 4653, were hybridized to the labeled viral RNA at 45°C overnight in Ambion hybridization buffer (Ambion Inc., Austin, Tex.). After hybridization, the RNA was digested with a mixture of RNases A (0.045 U/ml) and $T_1$ (1.8 U/ml) for 30 min at 37°C and then digested with proteinase K (130 μg/ml) for 15 min at 37°C (all enzymes from Boehringer), before being analyzed on a 2.4% Nusieve (FMC, Rockland, Maine) denaturing agarose gel. The gel was blotted as described above and analyzed on a PhosphorImager (Molecular Dynamics). The presence of a radiolabeled band of 178 nt indicated that the very 5′ end of the viral plus-strand RNA was synthesized during the pulse time and thus that plus-strand RNA synthesis had been initiated, whereas the presence of a band of 530 nt, originating from the middle region of the genome, indicated ongoing plus-strand RNA synthesis. As negative controls, hybridization was performed without added probe and after RNase digestion of the nascent plus strands of the RI.

**MAb.** The preparation and specificities of monoclonal antibodies (MAb) against 2C (40) and 14S (43) were described earlier. MAb against proteins 3D$^{pol}$ and 2B were prepared as described previously (40). As an antigen immunizing against protein 3D, a fusion protein of β-galactosidase and 3D expressed by the thermoinducible plasmid pEX2 in *Escherichia coli* NF1 was used. For induction of the MAb against 2B, the appropriate poliovirus sequence was PCR amplified, introduced in the IPTG (isopropyl-β-D-thiogalactopyranoside)-inducible vector DHRF, and expressed in *E. coli* M15. The expressed proteins were purified by polyacrylamide gel electrophoresis (PAGE) followed by electroelution (40) and Centriprep (Amicon, Danvers, Mass.) concentration. CBA mice and BALB/c mice were immunized with proteins 3D and 2B, respectively. The isolated spleen cells were restimulated in vitro with 1 to 5 μg of the appropriate antigen per ml during 3 days in the presence of interleukins 2, 4, 5, and 6 (a kind gift of P. Erb, Institute for Medical Microbiology, University of Basel) before being fused to SP2/0 cells with polyethylene glycol. The hybridoma supernatants were screened for MAb binding to their target proteins on Western blots (immunoblots) in order to select for sequence-specific MAb, which were previously found to be most suitable for immunocytochemistry (8).

**Immunoprecipitation and detergent treatment of vesicles.** For immunoprecipitation of native, non-detergent-treated vesicles, MACS beads (Miltenyi Biotec GmbH, Bergisch Gladbach, Germany) were used, since they allow direct examination of the precipitate by negative-staining EM and immuno-EM (IEM) because of their diameter of only 30 nm. For immunoprecipitation, 60 μl of rosettes was dissociated in 4 volumes of Tris (10 mM) and kept at 0°C for 15 min. Seventy microliters of MAb (hybridoma supernatant) was added, and after 30 min at 4°C, 10 μl of MACS (rat anti-mouse immunoglobulin G1-coated microbeads) was added and the incubation at 4°C was continued for another 15 min. Adsorption to, washing of, and elution from the magnetic column into 500 to 800 μl of 10 mM Tris buffer were done as indicated by the manufacturer.

For immunoprecipitation of detergent-treated vesicles, sheep anti-mouse antibody-coated magnetic beads (M 280; Dynal, Oslo, Norway) were used as described previously (42). For immunoprecipitation, detergents were added to the vesicles 15 min before the addition of the Dynabeads, and detergents were included in all incubation and washing steps. Final concentrations of detergents were 0.1 and 0.5% for Nonidet P-40 (NP-40) (Boehringer), 0.7% for Triton X-100 (Boehringer), and 0.2% for Na-deoxycholate (DOC) (Difco, Detroit, Mich.).

**PAGE and immunoblotting.** To analyze immunoprecipitated proteins, the precipitate was concentrated by acetone precipitation, dissolved in SDS-PAGE sample buffer, and loaded on an SDS-polyacrylamide gel (28). Blotting onto nitrocellulose filters was done as described by Towbin et al. (53). The blotted proteins were immunostained with our MAb, as indicated in Results, followed by peroxidase-coupled rabbit anti-mouse antibody.

**EM and EM-immunocytochemistry (IEM).** Dissociated or intact rosettes and their components as well as MACS-immunoprecipitated vesicles were processed for EM and IEM with our panel of MAb as described previously (14) with 5-nm-diameter colloidal gold particles coupled to goat antimouse antibody (Amersham) as a marker and 1% neutralized phosphotungstic acid as a stain. The preparations were viewed and photographed in a Siemens Elmiskop 102.

**RNase, ATA, and MAb treatment of vesicles.** In an attempt to specifically inhibit reassociation of vesicles into rosettes, the vesicles obtained by dissociating rosettes in the cold were treated either with 100 μg of RNase A (Boehringer) per ml at 25°C or with 100 μM aurintricarboxylic acid (ATA) (Sigma, St. Louis, Mo.) or MAb against 2C or 2B at 0°C for 15 min before being introduced in a cell-free transcription system. For these experiments, MAb from hybridomas grown in protein-free medium (Sigma) were partially purified and transferred into the HEPES (*N*-2-hydroxyethylpiperazine-*N*′-2-ethanesulfonic acid)-based in vitro transcription buffer by gel filtration through Bio-Spin 6 columns (Bio-Rad, Richmond, Calif.). MAb against 2B and 2C had the same concentration as measured by titration on dot blots. For some experiments, the MAb against 2C was concentrated 16 times by lyophilization.

## RESULTS

**Dissociation of rosettes and morphology of their components.** Upon isolation by cell fractionation and sucrose gradient centrifugation, the poliovirus replication complex presents itself as an RNA-synthesizing structure tightly enclosed in a rosette of virus-induced vesicles (14). In an attempt to investigate the architecture of such rosettes and the interplay of their components, we found the rosettes (Fig. 1a) to be dissociable into their components (Fig. 1b) by lowering of the temperature to 0°C and decreasing of the salt concentration from 150 mM to 30 to 40 mM by diluting the rosette-containing subcellular fraction with 10 mM Tris-HCl buffer or water. A low temperature was found to be more important for the dissociation process than a low salt concentration, since partial dissociation was obtained at 150 and 80 mM salt at 0°C. The dissociation of the rosettes was found to be reversible in that increasing the temperature to 30°C leads to reformation of rosettes (see below).

Negatively stained preparations of dissociated rosettes contain individual vesicles which carry pieces of a granular structure with an appearance very similar to that found in the center of the intact rosette and identified previously as the actual replication complex (11). These pieces are either capping the vesicles or covering small protrusions on the surface of the vesicles. The replication complex-like caps are also found to be associated with long tubules, of about 40 nm in diameter and 200 to 500 nm in length, emerging from many of the vesicles (Fig. 1c).

A much less frequently occurring population of vesicles has a diameter of approximately 50 nm (not shown). They correspond to the small, compact vesicles within the center of intact rosette described earlier (11). These small vesicles never were observed to carry any caps. Isolated larger replication complex-like structures like those obtained after DOC treatment of rosettes (11) are virtually never found.

**Immunocytochemical localization of viral proteins on the components of dissociated rosettes.** Previous IEM studies (10, 11, 14) have shown that the P2 proteins 2B and 2C and their precursors are located exclusively on the rosettes and thus can serve as marker proteins for the replication complex. IEM of dissociated isolated rosettes showed that all replication complex-like caps on the surface of the vesicles and tubules contain P2 proteins (Fig. 2a and b). 14S pentamer capsid precursors, which were previously shown to be abundant in the replication complex (42), were also found by IEM in many, albeit not all,

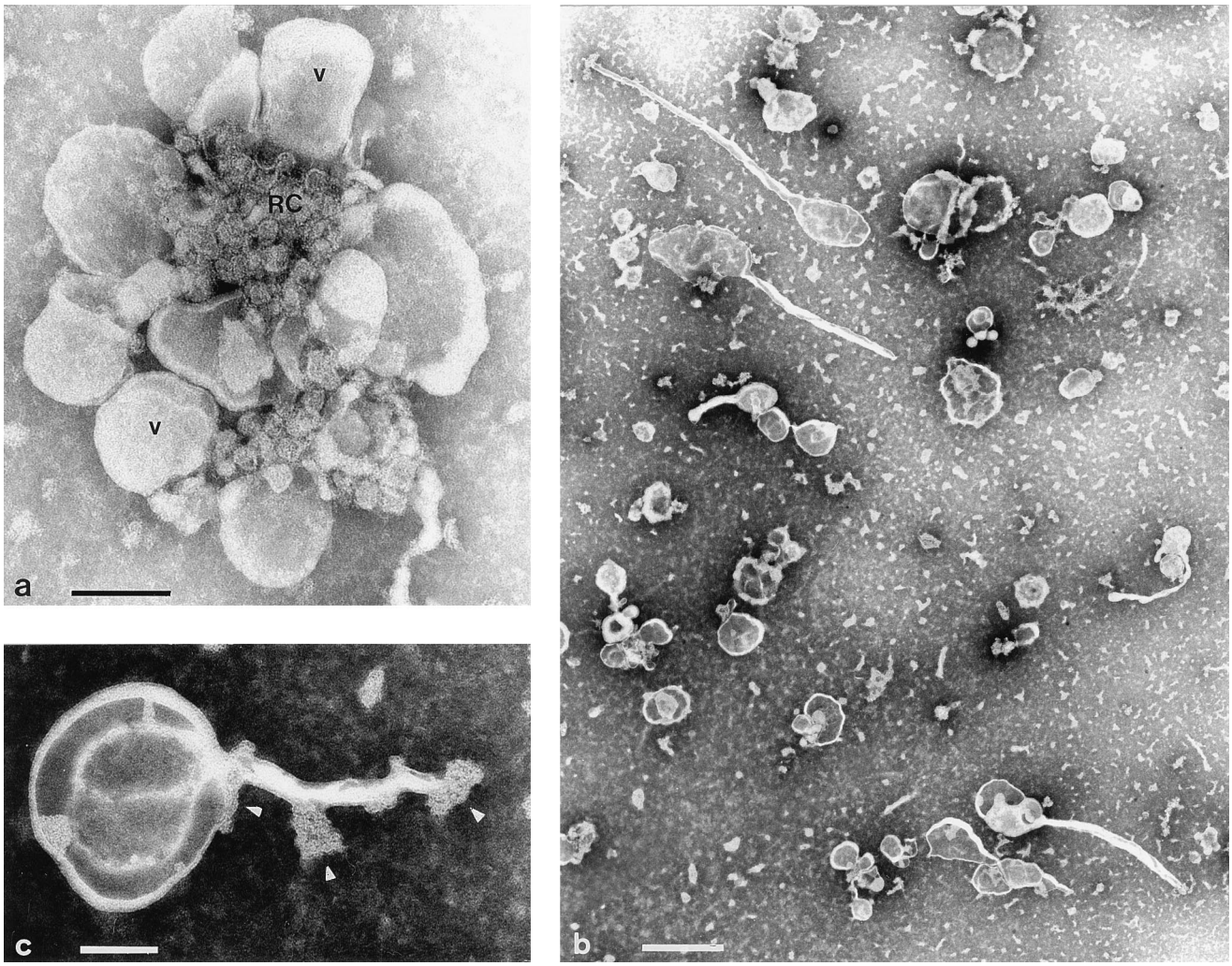


FIG. 1. (a) Rosette of virus-induced vesicles (V) surrounding a granular structure (RC) containing the replicating viral RNA, thus representing the actual replication complex. Such rosettes are isolated from infected cells by sucrose gradient centrifugation and synthesize viral plus-strand RNA in the RI in vitro. Bar, 100 nm. (b) Upon incubation at 0 to 4°C in low-ionic-strength buffer, rosettes dissociate into single vesicles. Bar, 500 nm. (c) Many of the vesicles carry tubules and pieces (caps [arrowheads]) of the granular replication complex. Bar, 100 nm.

of the caps (Fig. 2c). Labeling with the anti-3D MAb, however, was inconsistent and weak (not shown). It is not clear whether only some caps contain proteins with 3D epitopes or whether 3D is not easily accessible for immunolabeling. Alternatively, the caps could contain very small (i.e., catalytic) amounts of 3D.

The IEM experiments indicate that the caps consist of, or at least contain substantial amounts of, replication complex-derived material. The observations also indicate that dissociation of the rosette in the cold is fundamentally different from the dissociation of rosettes by guanidine (14). Guanidine, by interfering with protein 2C (44), detaches the replication complex from the vesicular membrane, thus giving rise to "naked" vesicles (14), whereas dissociation in the cold seems to break up the replication complex into pieces, which are still attached to the vesicular surface. In the following experiments, the protein and RNA contents of the caps were investigated.

**Immunoprecipitation of dissociated rosettes.** Native, dissociated rosettes were immunoprecipitated with the MACS system, and the precipitate was analyzed by IEM. The MAb directed against 2C, 2B, 3D, and 14S pentamers precipitated the same tubulated vesicles as observed in nonimmunoprecipitated dissociated rosettes (Fig. 3; compare with Fig. 1b and c and 2). Analysis of such precipitates on Western blots with a cocktail of our noncapsid MAb showed that all MAb precipitated, in addition to the proteins containing their own epitope, the entire set of P2 and P3 proteins recognized by the detection system (Fig. 4).

To test whether viral proteins are associated directly with each other or rather by virtue of the vesicular membrane, dissociated rosettes were detergent treated with either NP-40, Triton X-100, or DOC, and immunoprecipitation was carried out with Dynabeads. Under these conditions, the anti-P2 MAb no longer coprecipitated protein 3D (Fig. 5) and, inversely, the MAb against 3D did not coprecipitate the P2 proteins (Table 1), whereas the capsid proteins were found to remain associated with P2 proteins as well as with 3CD whether immunoprecipitation was done with MAb against 2B, 3D, or 14S (Table 1). This latter observation might also reflect an interaction

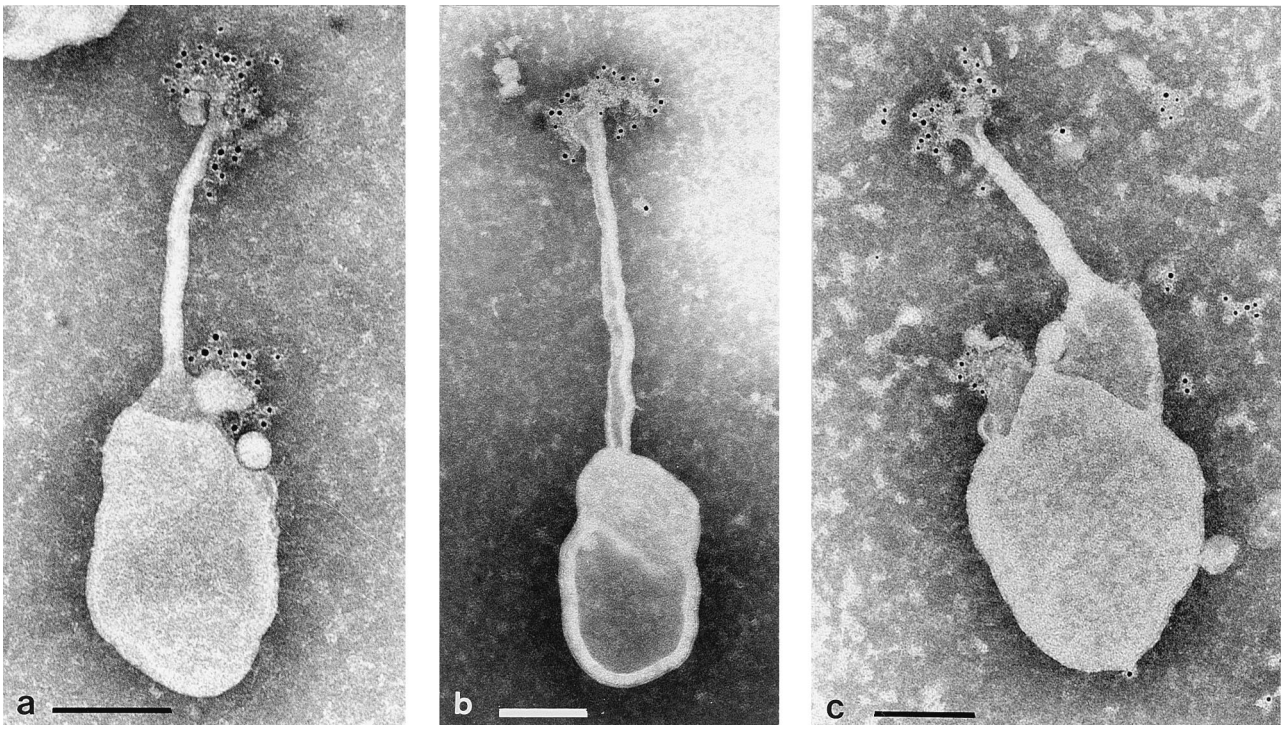


FIG. 2. IEM of single vesicles obtained by dissociation of rosettes in the cold. All caps were found to be labeled with MAb against 2C (a) and 2B (b), but only a subpopulation was labeled with MAb VP1, recognizing the 14S pentamer configuration (c). The non-vesicle-associated gold label in panel c represents free 14S pentamers. Bars, 100 nm.

of soluble 3CD (recognized by MAb against 3D) and 14S capsid proteins, as described previously (29).

**Viral RNA species associated with components of dissociated rosettes.** To test whether the viral RNA would be set free by the process of dissociation of the rosette, RNase was added to dissociated rosettes. The nascent plus strands on the RI

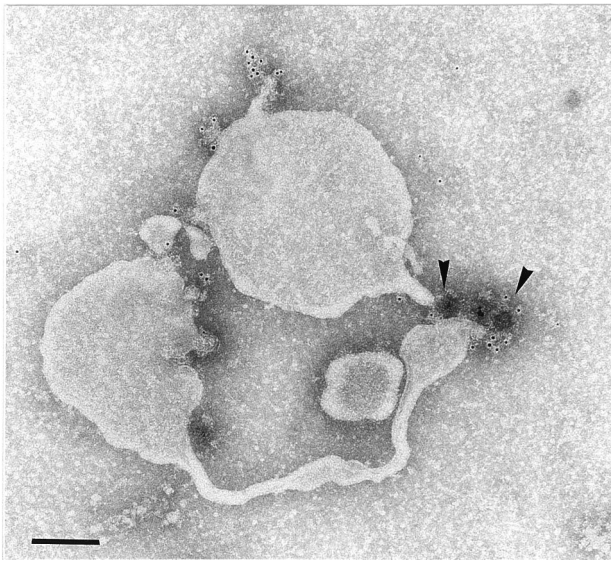

FIG. 3. IEM preparation of immunoprecipitate obtained from single vesicles of dissociated rosettes. MAb against 2B and MACS magnetic beads (arrowheads) precipitated tubulated vesicles identical to those shown in Fig. 2b. Bar, 100 nm.

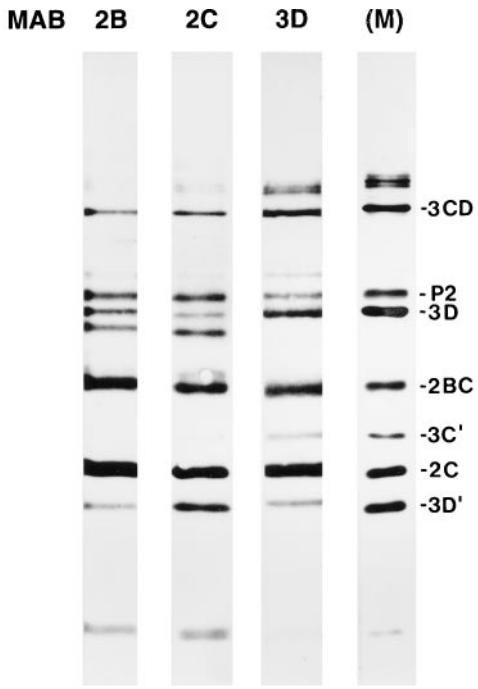


FIG. 4. Western blot of immunoprecipitate obtained with MACS magnetic beads as in Fig. 3 and MAb against 2B, 2C, and 3D. To test for coprecipitation of P2 and P3 viral proteins not recognized by the precipitating antibodies, the blot was developed with a cocktail of MAb against 2B and 2C and two MAb against 3D, one recognizing the N-terminal part of 3D, including 3C′, and one recognizing the C-terminal part of 3D, including 3D′. (M), poliovirus marker proteins.

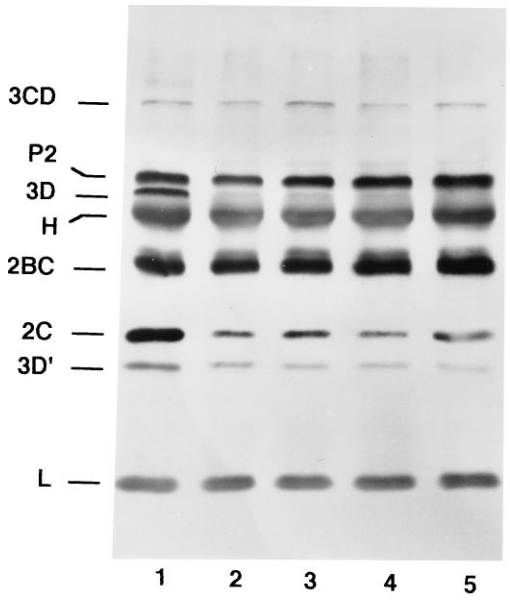


FIG. 5. Western blot of immunoprecipitates obtained from single vesicles of dissociated rosettes with Dynabeads and MAb against 2B. The vesicles were either not treated (lane 1) or detergent treated with 0.1% NP-40 (lane 2), 0.5% NP-40 (lane 3), 0.7% Triton X-100 (lane 4) or 0.2% DOC (lane 5) before and during immunoprecipitation. The blot was developed with the same cocktail of MAb as used for Fig. 4. Protein 3D no longer coprecipitated with the anti-2B MAb after detergent treatment. H and L, heavy and light chains of the precipitating MAb, respectively.

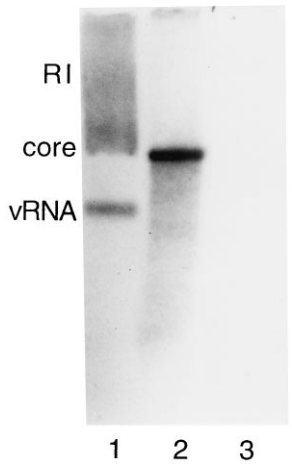


FIG. 6. After incubation for 60 min in an in vitro transcription system supplemented with [$^3$H]UTP, rosettes were dissociated at 0°C and either not treated (lane 1) or treated with RNase A (lane 2) or DOC and RNase A (lane 3). RNA was extracted, analyzed on a nondenaturing gel, En$^3$Hance impregnated, and fluorographed. Lane 1, UTP incorporation into the RI and genome-length RNA (vRNA); lane 2, vRNA and the nascent plus strands on the RI are RNase sensitive, so that only the core of the RI remains; lane 3, DOC renders all freshly synthesized RNA RNase sensitive.

were found to be RNase sensitive, and the RI was converted into core (18), whereas the entire RI was RNase sensitive only after DOC treatment of the vesicle preparation (Fig. 6). This suggested an association of the RI, or its core, with membranes.

Therefore, we wanted to know whether the RI would remain associated with individual capped vesicles when the rosette was in the dissociated state. To test this, dissociated rosettes were subjected to MACS immunoprecipitation with the MAb against 2B (Fig. 3). As shown above, endogenous RNase in the immunoprecipitation system can attack the nascent plus strands in the RI as soon as the rosette is dissociated. Thus, the RI was identified in 2B immunoprecipitates of dissociated rosettes by visualizing its 7.5-kb negative strand by Northern (RNA) blot hybridization with a minus-strand-detecting DIG-labeled riboprobe (Fig. 7, lane 3).

To confirm that the negative-strand RNA originated from RI molecules, we tested the RNase accessibility of the 7.5-kb minus strand before and after DOC treatment of dissociated rosettes (Fig. 6). Figure 7, lane 5, shows that the minus strand became RNase sensitive only after DOC treatment of single vesicles, which indicates that it was of RI origin associated with a single vesicle.

**Reassociation of vesicles into rosettes showing initiation and elongation activities.** Incubation of dissociated rosettes at 30°C causes a reassociation of the vesicles into rosettes as shown by IEM of such preparations. The vesicles become gradually tighter rosettes (Fig. 8), and in not yet completely reformed rosettes, the vesicles still carry their tubules, which seem to become interwoven, forming a tight network.

Figure 9A shows, on a nondenaturing RNA gel, that reassociated rosettes synthesize RNA, producing the same species of viral RNA as rosettes which have not been dissociated. To test whether the reassociated rosette not only elongates already initiated plus strands but also initiates viral plus-strand RNA synthesis, an RNase protection assay was performed (see Materials and Methods). Figure 9B, lane 1, shows that initiation as well as elongation is readily demonstrable after reassociation of vesicles into rosettes.

To test whether the initiation occurred on preformed initiation complexes, e.g., RNA-P3 protein-containing complexes as described previously (2, 3, 23), or whether such complexes were newly formed after rosette reassembly, reassociated rosettes were preincubated in an in vitro transcription system with unlabeled nucleoside triphosphates (NTPs) for 0, 30, or 60 min to use up preformed complexes. After that time, [$^{35}$S]UTP was added, and incubation was continued. Figure 9B, lanes 1, 3, and 4, show that with or without preincubation,

TABLE 1. Immunoprecipitation of native and detergent-treated vesicles

| Precipitating MAb | Proteins precipitated from: | |
|---|---|---|
| | Native vesicles | Detergent-treated vesicles |
| Anti-2B | 2BC, 2C, 3D, VP0, VP1, VP3 | 2BC, 2C, VP0, VP1, VP3 |
| Anti-2C | 2BC, 2C, 3D (VP NT[a]) | 2BC, 2C (VP NT) |
| Anti-3D | 2BC, 2C, 3CD, 3D, VP0, VP1, VP3 | 3CD, 3D, VP0, VP1, VP3 |
| Anti-14S pentamers | 2BC, 2C, 3CD, 3D, VP0, VP1, VP3 | 2BC, 2C, 3CD, VP0, VP1, VP3 |

[a] NT, not tested.

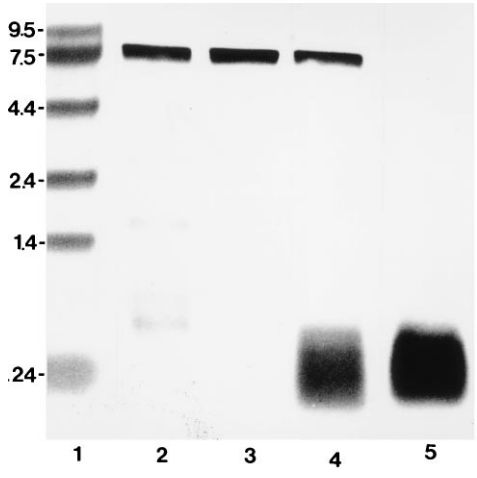


FIG. 7. Northern blot of immunoprecipitate obtained from single vesicles with MAb against 2B and MACS magnetic beads. The blot was probed with a DIG-labeled RNA probe (nt 163 to 443) of plus polarity. The blot shows that RI-derived minus strand is present in the 2B immunoprecipitate. Lane 1, marker; lanes 2 and 3, vesicles before (lane 2) and after (lane 3) immunoprecipitation contain 7.5-kb negative-strand RNA; lane 4, 7.5-kb negative-strand RNA in RNase-treated vesicles is still present; lane 5, in DOC- and RNase-treated vesicles, the 7.5-kb negative-strand RNA is RNase sensitive. Numbers on the left are sizes in kilobases.

syntheses of the 5′ end and central part of the plus strands were comparable. This argues for newly formed initiation complexes in the in vitro transcription system.

After the membranes were dissolved by DOC, however, synthesis of the 5′ ends of the viral plus strands was inhibited, whereas elongation in the P2 genomic region continued (Fig. 9B, lane 2). This is in agreement with earlier studies (11, 54) in which analysis of viral RNA synthesis showed that DOC-treated rosettes still elongate plus-strand RNA in the RI.

Neither reassociation, as determined by IEM, nor initiation and elongation (Fig. 9B, lane 5) could be inhibited by ATA, a drug known to prevent de novo protein-RNA interactions (15). Likewise, addition of purified MAb against 2C or 2B to dissociated rosettes before the temperature was raised to induce reassociation and RNA synthesis had no adverse effect on regaining of aspect and on the initiation and elongation activities of the rosettes (not shown). To test whether nascent viral plus-strand RNA would be involved directly or indirectly, e.g., via an RNA-associated protein(s), in reassociating vesicles to rosettes, dissociated rosettes were treated with RNase A to digest the nascent plus strands on the RI (Fig. 6). Upon raising of the temperature, the vesicles reassociated, as monitored by EM, and synthesized RNA (not shown). These results point to protein-lipid or protein-protein interactions as the driving force for the reassociation of vesicles into rosettes. However, since the functionality of the RI resides with individual vesicles, as shown below, reassociation and ongoing RNA synthesis are likely to be independent activities.

**Role of individual vesicles in RNA synthesis.** To test which steps in viral RNA synthesis (initiation or elongation) can be exerted by individual vesicles, 7 μl of rosettes was diluted, dissociated at 0°C, and then further diluted 20-fold into an in vitro transcription system containing [$^{35}$S]UTP. The vesicles were brought to 30°C to allow RNA synthesis to proceed. The purpose of the dilution of the vesicles was to prevent their reassociation during the rewarming and testing of their synthetic activity. This was confirmed by EM (not shown). Figure 10, lane 1, shows that viral plus-strand RNA was initiated and elongated. Analysis on native gels showed that [$^{35}$S]UTP was incorporated into the RI and genome-length RNA (not shown).

In contrast to the results of experiments in which vesicles were allowed to reassociate into intact rosettes (Fig. 9b), initiation but not elongation was sensitive to ATA in vesicles kept separated in the in vitro transcription system (Fig. 10, lane 2). This experiment indicates de novo formation of initiation complexes on individual vesicles. Thus, our findings show that individual vesicles are autonomous RNA-replicating units.

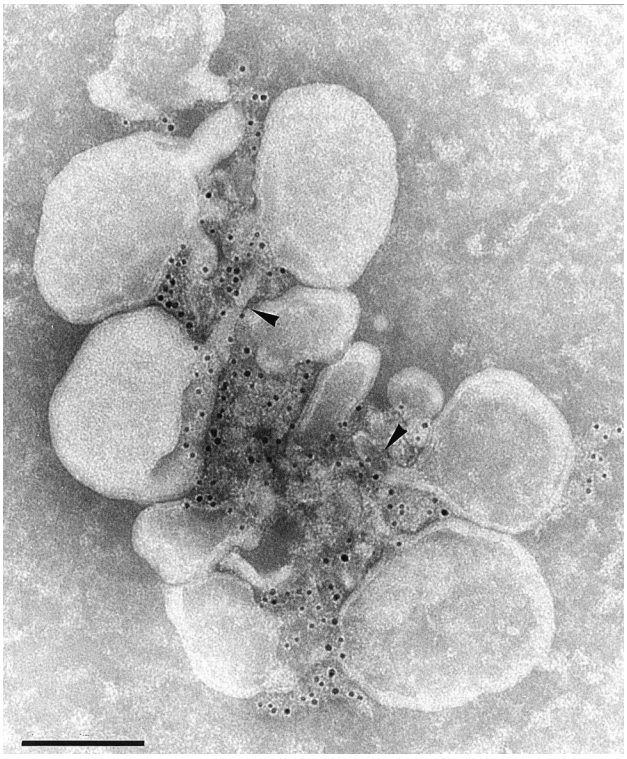

FIG. 8. Single vesicles from dissociated rosettes were incubated at 30°C. The IEM preparation (label, MAb against 2B) shows vesicles in the process of reassociation into a rosette. Note tubules (arrowheads) extending towards the center of the rosette. Bar, 100 nm.

## DISCUSSION

The multicomponent structure synthesizing poliovirus progeny plus-strand RNA in the infected cell is composed of virus-induced vesicles associated with the actual replication complex (14). Upon isolation, the vesicles are found to be arranged in rosettes, forming such a tight structure that it is difficult to get more insight into its architecture and functioning. Furthermore, the architectural integrity of the replication complex is generally considered necessary for its ability to replicate viral RNA (45). This notion stems from experiments in which the formation of vesicles was blocked by inhibitors such as Brefeldin A (25, 32) or Cerulenin (22) or in which the replication complex was disassembled with guanidine (14) or partially dissolved with detergents (11, 18, 54). The findings reported in this paper, i.e., not only that the rosette can be dissociated into single vesicles but also that the vesicles will spontaneously reform a rosette and that individual vesicles are capable of initiation and elongation of plus-strand RNA on their own, indicate that our protocol of dissociation of rosettes in the cold does not produce artifactual breakdown products but produces

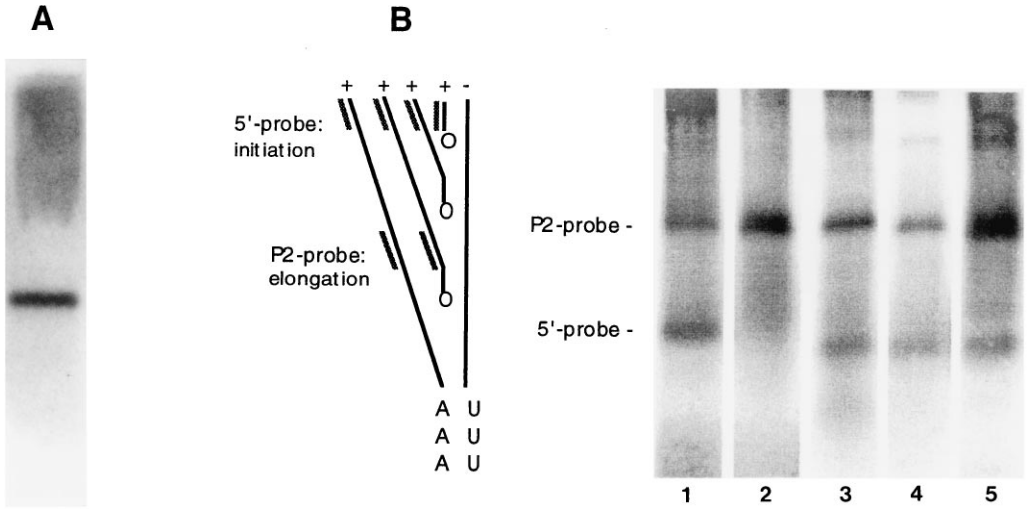


FIG. 9. (A) Reassociated rosettes (as in Fig. 8) were incubated for 60 min in an in vitro transcription system supplemented with [$^3$H]UTP and processed on a native gel as indicated in the legend to Fig. 6. UTP was incorporated into the RI and genome-length RNA. (B) Reassociated rosettes as in panel A. RNA was labeled with [$^{35}$S]UTP in an in vitro transcription system, extracted, and hybridized to unlabeled, minus-polarity riboprobes complementary to nt 1 to 178 to detect initiation and to nt 4124 to 4653 to detect elongation (see the schematic drawing and Materials and Methods). After RNase digestion, protected radiolabeled, and thus in vitro freshly synthesized, RNA bands were detected on blots of denaturing gels by PhosphoImager analysis. Lane 1, initiation and elongation in reassociated rosettes; lane 2, DOC added to vesicles during reassociation abolishes initiation but not elongation; lanes 3 and 4, reassociated rosettes were preincubated in an in vitro system with unlabeled NTPs for 30 and 60 min, respectively, and after preincubation, [$^{35}$S]UTP was added and incubation was continued. Lanes 1, 3, and 4 show comparable 5′ bands, used to detect initiation. Lane 5, single vesicles were treated with 100 μM ATA before being allowed to reassociate at 30°C in an in vitro system. In the rosette thus obtained, neither initiation nor elongation is blocked by ATA.

biologically meaningful subunits of the rosette and the replication complex. The analysis of these subunits might help to answer still-open questions about the structure and function of the replication complex.

A structural analysis of dissociated rosettes showed that their vesicles have tubular protrusions with parts of the replication complex attached to them. Upon reassociation, the protrusions extend inwards into the replication complex in the center of the rosette. It is not clear whether the tubules found with our virus-induced vesicles play any role in poliovirus RNA replication. Tubules with very similar structure and dimensions were found in isolated Golgi complexes (57; for a review, see reference 48), where their formation was inducible by the addition of NTPs and abolished by GTPγS. However, since poliovirus protein 2C was found to have ATP and GTP binding properties (34, 46) and to be able to induce extensive tubulation of membranes (17), it is tempting to speculate that the formation of the tubules might depend on NTP-binding and -hydrolyzing activities of protein 2C, satisfying structural needs of the RNA replication or the encapsidation step. Furthermore, similarity in the reactions of the Golgi membranes and of the virus-induced vesicles to GTP-binding proteins would not be surprising, since Schlegel et al. (49) have found Golgi membranes, as well as the endoplasmic reticulum, also to be involved in the formation of virus-induced vesicles.

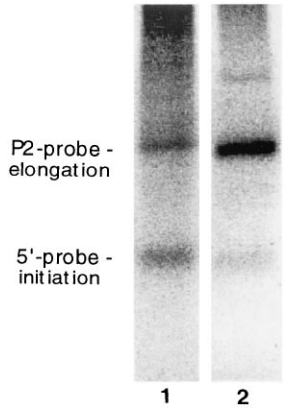


FIG. 10. After dissociation of rosettes, vesicles were kept single by high dilution in an in vitro transcription system at 30°C, and an RNA protection assay was performed as described for Fig. 9B to monitor initiation and elongation. Lane 1, single vesicles show initiation and elongation; lane 2, ATA greatly inhibits initiation on single vesicles.

Membranes of the virus-induced vesicles are not necessary for elongation of viral RNA but are required for initiation of viral plus-strand RNA synthesis (Fig. 9b). The membranes may not only act as a simple carrier for the initiation site, i.e., where the 3′ end of the minus-strand template comes together with viral and cellular proteins and structures participating in plus-strand initiation (2, 3, 23), but also organize and arrange all components involved in initiation so that the events making up initiation can proceed in a highly ordered way. Our approach to monitor this multistep initiation process was to demonstrate the synthesis of the very 5′ end of the viral plus strand, which is the consequence not only of the actual priming reaction but of all the other steps of initiation as well. Thus, synthesis of the 5′ ends of plus strands indicates that all initiation steps have successfully been accomplished.

Our immunoprecipitation experiments showed that the capsid proteins (14S pentamers), the P2 proteins 2C and 2BC, and the P3 proteins 3D and 3CD are coprecipitated from isolated native vesicles. It cannot be determined from this experiment if every cap contains all proteins. By IEM, all caps contain P2 but only some carry 14S pentamers or 3D or neither. This indicates that the vesicle population is heterogeneous in protein content. Preliminary experiments with an anti-3A MAb are consistent with such a heterogeneity (data not shown).

The association of the P2 proteins with each other and with the capsid proteins is detergent resistant, whereas the association of 3D$^{pol}$ with all other viral proteins tested in this assay

is detergent sensitive. This could mean either that $3D^{pol}$ is only loosely incorporated into caps or that it is not in the cap but only connected to it by virtue of the vesicular membrane. Since the actual location of $3D^{pol}$ could not be unambiguously determined by IEM, we do not know whether $3D^{pol}$, and hence the replication forks of the RI, are in any way attached to the caps or elsewhere to the vesicular surface.

In any case, immunoprecipitation showed the RI to be adsorbed to individual vesicles. RNase treatment indicated that after dissociation, the nascent plus strands of the RI are freely accessible for the enzyme, whereas the core with the replication forks is still protected. Conceivably, the RI would be adsorbed to the surface of the vesicular membrane and the replication forks additionally covered with protein. To allow the production of full-length genomic RNA on a single vesicle, the RI would have to be kept in an untangled configuration. However, the precise location of the RI on the vesicular surface still awaits further clarification.

If one assumes the distribution of viral proteins proposed above and of the RNA on the vesicular surface to reflect functional interactions, our findings would also indicate that the P2 proteins, in addition to their role in viral plus-strand RNA synthesis, participate in encapsidation (31).

Reassociation of vesicles into rosettes was not inhibited by MAb against 2C and 2B, by RNase digestion of the nascent plus strands on the RI, or by ATA. The ineffectiveness of the MAb in the inhibition of reassociation, despite the possible implication of the P2 proteins in the organization of the rosette (14), could be explained by the P2 proteins being already associated with their target, i.e., membranes. It is less likely that the epitope recognized by the MAb would be hidden under these conditions, since individual vesicles can be immunolabeled and immunoprecipitated with anti-P2 MAb.

The failure of ATA to prevent reassociation and, in reassociated vesicles, initiation is puzzling. While ongoing reassociation with ATA could be explained by RNA-protein interactions not being required for reassociation, initiation unquestionably involves such interactions. This is also shown by the finding that ATA greatly inhibits initiation in vesicles kept separately. However, if we take into account that the rosette protects the RI from RNase (11) and that Enviroxime (24) and guanidine (unpublished data) have no effect if added to in vitro RNA-synthesizing rosettes, a likely explanation for the lack of ATA-mediated inhibition of transcription in reassociated rosettes could be that early in reassociation the rosette becomes impermeable also to ATA so that the amount of the drug present within the rosette becomes insufficient to block initiation.

A hypothetical model of the rosette's architecture put forward earlier (11) calls for an RI stretched out within a rosette with its 5′ ends of the nascent plus strands attached to the surface of the rosette's vesicles. However, the observation that RNase digestion of the nascent 5′ ends in the RI does not inhibit reassociation indicates that nascent plus strands do not seem to be involved in (re-)association of vesicles into rosettes.

Clearly, the vesicles seem to have a strong tendency to reform rosettes, even though the mechanism of reassociation is not known. To form a rosette could be advantageous for virus replication because it could greatly increase the effectiveness and speed of plus-strand RNA synthesis. There are two main reasons for this: first, macromolecular crowding, exerted by the mass of vesicles, leading to an enhanced concentration of factors necessary for RNA synthesis; and second, the providing of more membrane-bound initiation sites (20, 23) for the RI. This allows the RI, or rather its minus-strand template RNA, to easily move on within the rosette and to combine with its 3′ end with the next initiation site on the same or the next vesicle. This would make the rosette, as such, a higher-order structure with functional subunits (vesicles), although in the infected cell the rosette could well be a short-lived, transient structure, changing its framework of individual vesicles continuously as the 3′ end of the minus strand moves on.

## ACKNOWLEDGMENTS

This work was supported by a grant (31-39175.93) from the Swiss National Science Foundation.

We thank Gaby Schaub for technical assistance and Andrea Ruhm for help with the preparation of MAb.

## REFERENCES

1. **Aldabe, R., and L. Carrasco.** 1995. Induction of membrane proliferation by poliovirus proteins 2C and 2BC. Biochem. Biophys. Res. Commun. **206:**64–76.
2. **Andino, R., G. E. Rieckhof, P. L. Achacoso, and D. Baltimore.** 1993. Poliovirus RNA synthesis utilizes an RNP complex formed around the 5′ end of viral RNA. EMBO J. **12:**3587–3598.
3. **Andino, R., G. E. Rieckhof, and D. Baltimore.** 1990. A functional ribonucleoprotein complex forms around the 5′ end of poliovirus RNA. Cell **63:**369–380.
4. **Baron, M. H., and D. Baltimore.** 1982. In vitro copying of viral positive strand RNA by poliovirus replicase. Characterization of the reaction and its products. J. Biol. Chem. **257:**12359–12366.
5. **Barton, D. J., P. E. Black, and J. B. Flanegan.** 1995. Complete replication of poliovirus in vitro: preinitiation RNA replication complexes require soluble cellular factors for the synthesis of Vpg-linked RNA. J. Virol. **69:**5516–5527.
6. **Barton, D. J., and J. B. Flanegan.** 1993. Coupled translation and replication of poliovirus RNA in vitro: synthesis of functional 3D polymerase and infectious virus. J. Virol. **67:**822–831.
7. **Bernstein, H. D., P. Sarnow, and D. Baltimore.** 1986. Genetic complementation among poliovirus mutants derived from an infectious cDNA clone. J. Virol. **60:**1040–1049.
8. **Bienz, K., D. Egger, and L. Pasamontes.** 1986. Electron microscopic immunocytochemistry. Silver enhancement of colloidal gold marker allows double labeling with the same primary antibody. J. Histochem. Cytochem. **34:**1337–1342.
9. **Bienz, K., D. Egger, and L. Pasamontes.** 1987. Association of polioviral proteins of the P2 genomic region with the viral replication complex and virus-induced membrane synthesis as visualized by electron microscopic immunocytochemistry and autoradiography. Virology **160:**220–226.
10. **Bienz, K., D. Egger, and T. Pfister.** 1994. Characteristics of the poliovirus replication complex. Arch. Virol. Suppl. **9:**147–157.
11. **Bienz, K., D. Egger, T. Pfister, and M. Troxler.** 1992. Structural and functional characterization of the poliovirus replication complex. J. Virol. **66:**2740–2747.
12. **Bienz, K., D. Egger, Y. Rasser, and W. Bossart.** 1980. Kinetics and location of poliovirus macromolecular synthesis in correlation to virus-induced cytopathology. Virology **100:**390–399.
13. **Bienz, K., D. Egger, Y. Rasser, and W. Bossart.** 1983. Intracellular distribution of poliovirus proteins and the induction of virus-specific cytoplasmic structures. Virology **131:**39–48.
14. **Bienz, K., D. Egger, M. Troxler, and L. Pasamontes.** 1990. Structural organization of poliovirus RNA replication is mediated by viral proteins of the P2 genomic region. J. Virol. **64:**1156–1163.
15. **Blumenthal, T., and T. A. Landers.** 1973. The inhibition of nucleic acid-binding proteins by aurintricarboxylic acid. Biochem. Biophys. Res. Commun. **55:**680–688.
16. **Caliguiri, L. A., and I. Tamm.** 1970. The role of cytoplasmic membranes in poliovirus biosynthesis. Virology **42:**100–111.
17. **Cho, M. W., N. Teterina, D. Egger, K. Bienz, and E. Ehrenfeld.** 1994. Membrane rearrangement and vesicle induction by recombinant poliovirus 2C and 2BC in human cells. Virology **202:**129–145.
18. **Etchison, D., and E. Ehrenfeld.** 1981. Comparison of replication complexes synthesizing poliovirus RNA. Virology **111:**33–46.
19. **Flanegan, J. B., and D. Baltimore.** 1979. Poliovirus polyuridilic acid polymerase and RNA replicase have the same viral polypeptide. J. Virol. **29:**352–360.
20. **Giachetti, C., and B. L. Semler.** 1991. Role of a membrane polypeptide in strand-specific initiation of poliovirus RNA synthesis. J. Virol. **65:**2647–2654.
21. **Girard, M.** 1969. In vitro synthesis of poliovirus ribonucleic acid: role of the replicative intermediate. J. Virol. **3:**376–384.
22. **Guinea, R., and L. Carrasco.** 1990. Phospholipid biosynthesis and poliovirus genome replication, two coupled phenomena. EMBO J. **9:**2011–2016.
23. **Harris, K. S., W. Xiang, L. Alexander, W. S. Lane, A. V. Paul, and E. Wimmer.** 1994. Interaction of poliovirus polypeptide 3CDpro with the 5′ and 3′ termini of the poliovirus genome. J. Biol. Chem. **269:**27004–27014.

24. **Heinz, B. A., and L. M. Vance.** 1995. The antiviral compound Enviroxime targets the 3A coding region of rhinovirus and poliovirus. J. Virol. **69:**4189–4197.
25. **Irurzun, A., L. Perez, and L. Carrasco.** 1992. Involvement of membrane traffic in the replication of poliovirus genomes. Effects of Brefeldin A. Virology **191:**166–175.
26. **Johnson, K. L., and P. Sarnow.** 1991. Three poliovirus 2B mutants exhibit noncomplementable defects in viral RNA amplification and display dosage-dependent dominance over wild-type poliovirus. J. Virol. **65:**4341–4349.
27. **Kuhn, R. J., H. Tada, F. Ypma-Wong, J. J. Dunn, B. L. Semler, and E. Wimmer.** 1988. Construction of a "mutagenesis cartridge" for poliovirus genome-linked viral protein: isolation and characterization of viable and nonviable mutants. Proc. Natl. Acad. Sci. USA **85:**519–523.
28. **Laemmli, U. K.** 1970. Cleavage of structural proteins during the assembly of the head of bacteriophage T4. Nature (London) **227:**680–685.
29. **Lawson, M. A., and B. L. Semler.** 1992. Alternate poliovirus nonstructural protein processing cascades generated by primary sites of 3C-proteinase cleavage. Virology **191:**309–320.
30. **Li, J.-P., and D. Baltimore.** 1988. Isolation of poliovirus 2C mutants defective in viral RNA synthesis. J. Virol. **62:**4016–4021.
31. **Li, J.-P., and D. Baltimore.** 1990. An intragenic revertant of a poliovirus 2C mutant has an uncoating defect. J. Virol. **64:**1102–1107.
32. **Maynell, L. A., K. Kirkegaard, and M. W. Klymkowsky.** 1992. Inhibition of poliovirus RNA synthesis by Brefeldin A. J. Virol. **66:**1985–1994.
33. **McBride, A. E., A. Schlegel, and K. Kirkegaard.** 1996. Human protein Sam 68 relocalization and interaction with poliovirus RNA polymerase in infected cells. Proc. Natl. Acad. Sci. USA **93:**2296–2301.
34. **Mirzayan, C., and E. Wimmer.** 1994. Biochemical studies on poliovirus polypeptide 2C: evidence for ATPase activity. Virology **199:**176–187.
35. **Molla, A., K. S. Harris, A. V. Paul, S. H. Shin, J. Mugavero, and E. Wimmer.** 1994. Stimulation of poliovirus proteinase 3Cpro-related proteolysis by the genome-linked protein VPg and its precursor 3AB. J. Biol. Chem. **269:**27015–27020.
36. **Molla, A., A. V. Paul, M. Schmid, S. K. Jang, and E. Wimmer.** 1993. Studies on dicistronic polioviruses implicate viral proteinase 2A (pro) in RNA replication. Virology **196:**739–747.
37. **Molla, A., A. V. Paul, and E. Wimmer.** 1991. Cell-free, de novo synthesis of poliovirus. Science **254:**1647–1651.
38. **Molla, A., A. V. Paul, and E. Wimmer.** 1993. Effects of temperature and lipophilic agents on poliovirus formation and RNA synthesis in a cell-free system. J. Virol. **67:**5932–5938.
39. **Mosser, A. G., L. A. Caliguiri, and I. Tamm.** 1972. Incorporation of lipid precursors into cytoplasmic membranes of poliovirus-infected Hela cells. Virology **47:**39–47.
40. **Pasamontes, L., D. Egger, and K. Bienz.** 1986. Production of monoclonal and monospecific antibodies against non-capsid proteins of poliovirus. J. Gen. Virol. **67:**2415–2422.
41. **Paul, A. V., X. Cao, K. S. Harris, J. Lama, and E. Wimmer.** 1994. Studies with poliovirus polymerase 3Dpol. Stimulation of poly(U) synthesis in vitro by purified poliovirus protein 3AB. J. Biol. Chem. **269:**29173–29181.
42. **Pfister, T., D. Egger, and K. Bienz.** 1995. Poliovirus subviral particles associated with progeny RNA in the replication complex. J. Gen. Virol. **76:**63–71.
43. **Pfister, T., L. Pasamontes, M. Troxler, D. Egger, and K. Bienz.** 1992. Immunocytochemical localization of capsid-related particles in subcellular fractions of poliovirus-infected cells. Virology **188:**676–684.
44. **Pincus, S. E., and E. Wimmer.** 1986. Production of guanidine-resistant and -dependent poliovirus mutants from cloned cDNA: mutations in polypeptide 2C are directly responsible for altered guanidine sensitivity. J. Virol. **60:**793–796.
45. **Plotch, S. J., and O. Palant.** 1995. Poliovirus protein 3AB forms a complex with and stimulates the activity of the viral RNA polymerase, 3D pol. J. Virol. **69:**7169–7179.
46. **Rodriguez, P. L., and L. Carrasco.** 1993. Poliovirus protein-2C has ATPase and GTPase activities. J. Biol. Chem. **268:**8105–8110.
47. **Roehl, H. H., and B. L. Semler.** 1995. Poliovirus infection enhances the formation of two ribonucleoprotein complexes at the 3′ end of viral negative-strand RNA. J. Virol. **69:**2954–2961.
48. **Rothman, J. E.** 1994. Mechanisms of intracellular protein transport. Nature (London) **372:**55–63.
49. **Schlegel, A., T. H. Giddings, Jr., M. S. Ladinsky, and K. Kirkegaard.** 1996. Cellular origin and ultrastructure of membranes induced during poliovirus infection. J. Virol. **70:**6576–6588.
50. **Sitzmann, J. H., and P. K. Lemotte.** 1993. Rapid and efficient generation of PCR-derived riboprobe templates for in situ hybridization histochemistry. J. Histochem. Cytochem. **41:**773–776.
51. **Takeda, N., R. J. Kuhn, C.-F. Yang, T. Takegami, and E. Wimmer.** 1986. Initiation of poliovirus plus-strand RNA synthesis in a membrane complex of infected HeLa cells. J. Virol. **60:**43–53.
52. **Teterina, N. L., W. D. Zhou, M. W. Cho, and E. Ehrenfeld.** 1995. Inefficient complementation activity of poliovirus 2C and 3D proteins for rescue of lethal mutants. J. Virol. **69:**4245–4254.
53. **Towbin, H., T. Staehelin, and J. Gordon.** 1979. Electrophoretic transfer of proteins from polyacrylamide gels to nitrocellulose sheets: procedure and some applications. Proc. Natl. Acad. Sci. USA **76:**4350–4354.
54. **Toyoda, H., C. F. Yang, N. Takeda, A. Nomoto, and E. Wimmer.** 1987. Analysis of RNA synthesis of type 1 poliovirus by using an in vitro molecular genetic approach. J. Virol. **61:**2816–2822.
55. **VanDyke, T. A., and J. B. Flanegan.** 1980. Identification of poliovirus polypeptide p63 as a soluble RNA-dependent RNA polymerase. J. Virol. **35:**732–740.
56. **VanKuppeveld, F. J. M., J. M. D. Galama, J. Zoll, P. J. J. vandenHurk, and W. J. G. Melchers.** 1996. Coxsackie B3 virus protein 2B contains a cationic amphipathic helix that is required for viral RNA replication. J. Virol. **70:**3876–3886.
57. **Weidman, P., R. Roth, and J. Heuser.** 1993. Golgi membrane dynamics imaged by freeze-etch electron microscopy. Views of different membrane coatings involved in tubulation versus vesiculation. Cell **75:**123–133.
58. **Young, I. D., R. J. Stewart, L. Ailles, A. Mackie, and J. Gore.** 1993. Synthesis of digoxigenin-labeled cRNA probes for nonisotopic in situ hybridization using reverse transcription polymerase chain reaction. Biotech. Histochem. **68:**153–158.